

COLOR-SELECTED GALAXIES AT $z \approx 6$ IN THE GREAT OBSERVATORIES ORIGINS DEEP SURVEY¹

M. DICKINSON,² D. STERN,³ M. GIAVALISCO,² H. C. FERGUSON,² Z. TSVETANOV,⁴ R. CHORNOCK,⁵ S. CRISTIANI,⁶ S. DAWSON,⁵ A. DEY,⁷ A. V. FILIPPENKO,⁵ L. A. MOUSTAKAS,² M. NONINO,⁶ C. PAPOVICH,⁸ S. RAVINDRANATH,² A. RIESS,² P. ROSATI,⁹ H. SPINRAD,⁵ AND E. VANZELLA^{9,10}

Received 2003 May 28; accepted 2003 October 31; published 2004 January 9

ABSTRACT

We report early results on galaxies at $z \sim 6$ selected from *Hubble Space Telescope* imaging for the Great Observatories Origins Deep Survey. Spectroscopy of one object with the Advanced Camera for Surveys grism and from the Keck and Very Large Telescope observatories shows a strong continuum break and asymmetric line emission, identified as Ly α at $z = 5.83$. We find only five spatially extended candidates with signal-to-noise ratios greater than 10, two of which have spectroscopic confirmation. This is much fewer than would be expected if galaxies at $z = 6$ had the same luminosity function as those at $z = 3$. There are many fainter candidates, but we expect substantial contamination from foreground interlopers and spurious detections. Our best estimates favor a $z = 6$ galaxy population with fainter luminosities, higher space density, and similar comoving ultraviolet emissivity to that at $z = 3$, but this depends critically on counts at fluxes fainter than those reliably probed by the current data.

Subject headings: early universe — galaxies: evolution — galaxies: formation — galaxies: high-redshift

On-line material: machine-readable table

1. INTRODUCTION

Broadband color selection, based on ultraviolet (UV) spectral breaks caused by neutral hydrogen, is an efficient technique for identifying galaxies at $z = 3$ –4 (Steidel et al. 1996; Madau et al. 1996). At higher redshifts and relatively bright magnitudes, $i' - z'$ colors from the Sloan Digital Sky Survey have been used to identify QSOs out to $z = 6.4$ (Fan et al. 2003). Some galaxies at $z > 5$ have also been found in this way, but the required deep imaging and spectroscopy is extremely challenging. A Lyman break galaxy (LBG) with typical (L^*) UV luminosity at $z = 3$ ($M_{1700\text{\AA}} = -21.0$; Adelberger & Steidel 2000) would have $m(z) = 26.0$ if moved, without evolution, to $z = 6$ and would be undetected in the i band (hence, an “ i -dropout”). At $z \geq 6.5$, Ly α shifts through the z band, and galaxies are lost to optical sight altogether.

One goal of the Great Observatories Origins Deep Survey (GOODS) is to find and study large numbers of galaxies at $3.5 < z < 6.5$. Here we report initial results on galaxy candi-

dates at $z \sim 6$, including spectroscopy for one galaxy, CDFS J033240.0–274815 (hereafter SiD2). We use AB magnitudes ($AB \equiv 31.4 - 2.5 \log \langle f_\nu/nJy \rangle$) and assume a cosmology with $\Omega_{\text{tot}}, \Omega_M, \Omega_\Lambda = 1.0, 0.3, 0.7$ and $H_0 = 70 \text{ km s}^{-1} \text{ Mpc}^{-1}$.

2. IMAGING, PHOTOMETRY, AND COLOR SELECTION

The GOODS Treasury Program covers areas around the Chandra Deep Field–South (CDF-S) and Hubble Deep Field–North (HDF-N) with mosaics of Advanced Camera for Surveys (ACS) images. The observations, data reduction, and catalogs are described in Giavalisco et al. (2004b). Our present analysis uses three-epoch co-added images for both fields, with 3, 1.5, 1.5, and 3 orbit depth in the F435W, F606W, F775W, and F850LP filters (hereafter $B_{435}, V_{606}, i_{775},$ and z_{850} , respectively). After discarding regions near the image borders or without four-band coverage, the survey solid angle is 316 arcmin^2 . We detect objects in the z_{850} images using SExtractor (Bertin & Arnouts 1996), and we measure photometry through matched apertures in all bands. Here we use z_{850} “total” magnitudes (SExtractor MAG_AUTO), and colors measured through isophotal apertures defined in the z_{850} image.

We estimate the reddest colors expected for ordinary galaxies with spectral templates (Coleman, Wu, & Weedman 1980) integrated through the ACS bandpasses. The redshifted colors of an elliptical galaxy peak¹¹ at $i_{775} - z_{850} \approx 1.2$ for $z \approx 1.1$. There is only one “bright” galaxy in the GOODS fields with $i_{775} - z_{850} > 1.3$ ($z_{850} = 23.9$; $i_{775} - z_{850} = 1.32$). It is well detected at V_{606} , bright in the near-infrared (IR), and certainly has $z \ll 6$. Redder colors may be explained by dust obscuration, high metallicity, strong line emission in the z_{850} band, or intergalactic medium (IGM) absorption at high redshift. For the range of UV colors for LBGs at $z \approx 3$, $i_{775} - z_{850} > 1.3$ is crossed at $z = 5.5$ – 5.7 . Cool stars may also be this red, but only a tiny minority of high-latitude stars have $i' - z' > 1.3$ (Fan et al.

¹ Based on observations taken with the NASA/ESA *Hubble Space Telescope*, which is operated by AURA, Inc., under NASA contract NAS5-26555, the W. M. Keck Observatories, and the Very Large Telescope (VLT) at Cerro Paranal, Chile, operated by the European Southern Observatory, under programs 170.A-0788 and 168.A-0485.

² Space Telescope Science Institute (STScI), 3700 San Martin Drive, Baltimore, MD 21218.

³ Jet Propulsion Laboratory, California Institute of Technology, Mail Stop 169-506, Pasadena, CA 91109.

⁴ Department of Physics and Astronomy, Johns Hopkins University, 3400 North Charles Street, Baltimore, MD 21218-2686.

⁵ Department of Astronomy, University of California, Berkeley, Mail Code 3411, Berkeley, CA 94720.

⁶ Istituto Nazionale di Astrofisica, Osservatorio Astronomico di Trieste, via G. B. Tiepolo 11, Trieste I-34131, Italy.

⁷ National Optical Astronomical Observatory, 950 North Cherry Avenue, Tucson, AZ 85719.

⁸ Steward Observatory, University of Arizona, 933 Cherry Avenue, Tucson, AZ 85721-0065.

⁹ European Southern Observatory, Karl-Schwarzschild-Strasse 2, D-85748 Garching bei München, Germany.

¹⁰ Dipartimento di Astronomia dell’Università di Padova, Vicolo dell’Osservatorio 2, I-35122 Padua, Italy.

¹¹ The redshifted elliptical template has redder colors at $1.7 < z < 2.3$, but the UV spectrum of any galaxy at that redshift is unlikely to resemble that of an old elliptical galaxy at $z \approx 0$.

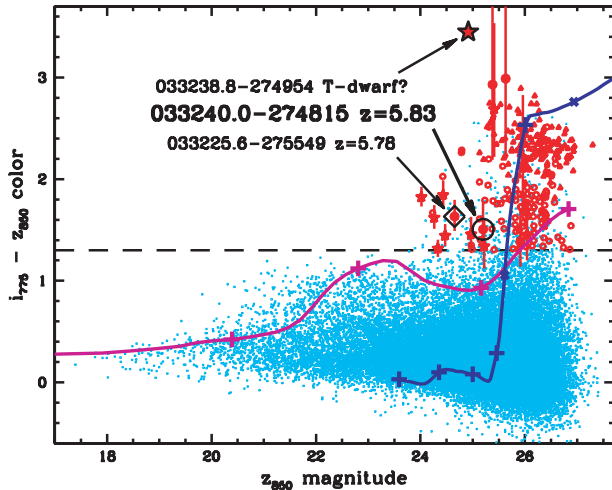


FIG. 1.—Color-magnitude diagram for the combined GOODS fields. The dashed line shows our i -dropout color selection limit. Light blue points are extended objects that do not meet the color and $S/N(B_{435}, V_{606}) < 2$ criteria. Triangles mark 1σ lower color limits for objects undetected in i_{775} . Red circles are i -dropout candidates. The larger, filled circles with error bars (1σ) are candidates with $S/N(z_{850}) > 10$; stars mark point sources. Two galaxies with spectroscopic redshifts are highlighted, as is a possible T dwarf. The mauve curve shows the color-magnitude track for an unevolving, L^* elliptical galaxy; vertical crosses mark $z = 0.5, 1, 1.5$ and 2.0 . The blue curve shows the track for an unevolving $L_{z=3}^+$ LBG with average UV colors; vertical crosses mark $z = 2, 3, 4, 5$, and 6 , while mult crosses mark $z = 5.5$ and 6.5 .

2003), and our ACS imaging provides a robust measure of stellarity for $z_{850} < 26.2$.

The three-epoch ACS mosaics have very small misalignments between images, and these misalignments can trigger over-rejection in the cores of point sources during cosmic-ray removal in the V_{606} and i_{775} bands (only the B_{435} and z_{850} images are reduced differently). There is virtually no photometric impact for extended sources, but the $i_{775}-z_{850}$ colors of brighter stars can be biased redward, and we treat them with caution here.

We are interested in objects near our detection limits. The signal-to-noise ratio (S/N) of a measurement depends on the source flux and size and on the exposure time, which varies with position in our mosaics. The significance of a source is best estimated not from its magnitude but from $S/N(z_{850})$ in the detection aperture. Our photometric errors are computed from noise maps that account for interpixel correlations. To verify their reliability, we added artificial objects to the z_{850} images (only) and detected them with SExtractor. Background-subtracted counts (S_i) were measured through matched apertures for the other bands and compared with the predicted uncertainties (σ_i) from the noise maps. The distribution of S_i/σ_i is nearly Gaussian with a mode of ≈ 0 and an rms of ≈ 1 , showing that our error estimates are reliable, except for a positive tail due to blending with other objects. Because of this tail, 14% of $z \sim 6$ galaxies would have $S/N > 2$ in the B_{435} or V_{606} bands.¹² We consider this an acceptable loss rate and adopt $i_{775}-z_{850} > 1.3$ and $S/N(B_{435}, V_{606}) < 2$ as our i -dropout criteria (Fig. 1).

3. SPECTROSCOPY

Supernovae found by GOODS are studied in a Target-of-Opportunity program that, in some cases, obtains low-resolution, slitless spectra with the ACS G800L grism. An 18,840 s

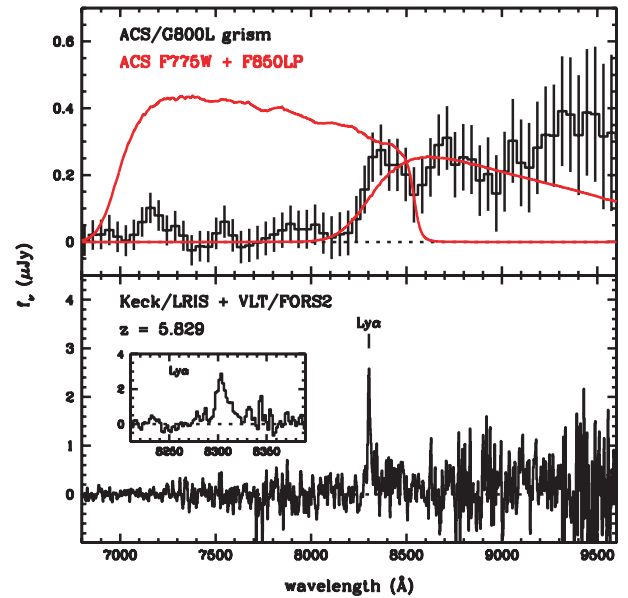


FIG. 2.—*Top*: ACS grism spectrum of SiD2. Pixels in the spectrum are correlated by the data reduction process and thus have smaller scatter than suggested by the 1σ error bars. The curves show unnormalized bandpass functions for the i_{775} and z_{850} filters. *Bottom*: Keck+VLT spectrum of SiD2, slightly smoothed. The inset panel shows a magnified (unsmoothed) view of the Ly α emission line.

G800L observation of SN 2002FW (Riess et al. 2004) was obtained on UT 2002 October 1 and included SiD2. It was reduced with the CALACS pipeline and the aXe extraction software. The spectrum (Fig. 2, *top*) shows a flat continuum with a sharp break at $\lambda \approx 8300$ Å.

We observed SiD2 with the Low Resolution Imaging Spectrometer (LRIS; Oke et al. 1995) on the Keck I telescope on

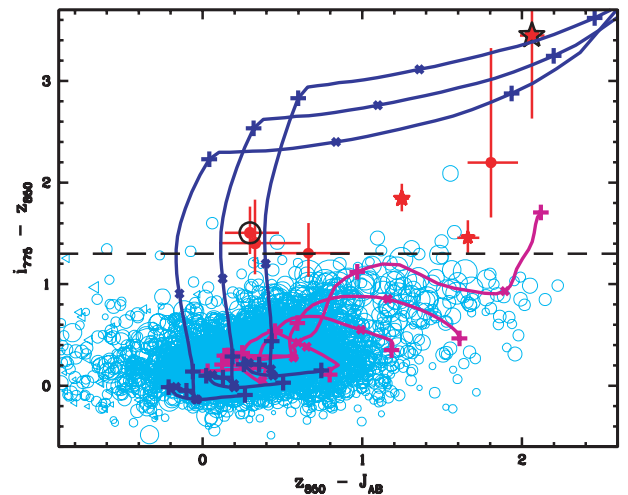


FIG. 3.—Optical-infrared two-color diagram for a portion of the CDF-S (using ISAAC near-IR data). The circles show objects with $S/N(z) > 7$, with sizes proportional to their J magnitudes. The filled circles and stars with error bars (1σ) are objects (extended and unresolved) that meet our i -dropout criteria. The filled red circle for SiD2 is circled in black. Open circles show extended objects that do not meet these criteria. The mauve curves show modeled colors of ordinary, low-redshift galaxies, redshifted over $0 < z < 2$. The blue curves show the expected colors of LBGs at $2 < z < 7$ ($z = 6$ at the “bend”), spanning the range of UV spectral slopes seen in LBGs at $z \approx 3$. The crosses on the curves mark the same redshifts as in Fig. 1.

¹² On average, this limit corresponds to $B_{435} > 29.1$ or $V_{606} > 29.1$.

TABLE 1
THE $z \sim 6$ GALAXY CANDIDATES, ORDERED BY $S/N(z_{850})^a$

ID	R.A. (J2000)	Decl. (J2000)	$S/N(z_{850})$	$m(z_{850})$	$i_{775}-z_{850}^b$	FWHM(z_{850}) (arcsec)	Notes
SiD001	03 32 25.60	-27 5548.6	20.45	24.65 ± 0.06	1.63 ± 0.15	0.18	SBM object 3, $z = 5.78$ (Bunker et al. 2003)
SiD002	03 32 40.02	-27 48 15.0	12.72	25.20 ± 0.12	1.51 ± 0.23	0.19	SBM object 1, $z = 5.83$ (this Letter); ISAAC
SiD003	03 32 19.07	-27 54 21.9	11.72	25.91 ± 0.13	1.39 ± 0.28	0.27	SBM object 7; faint IR (SOFI)
NiD001	12 36 19.90	62 09 34.2	10.55	25.63 ± 0.13	>2.29	0.19	
SiD004	03 32 33.20	-27 39 49.2	10.24	25.38 ± 0.13	>2.21	0.70	Faint IR (SOFI)

NOTE.—Units of right ascension are hours, minutes, and seconds, and units of declination are degrees, arcminutes, and arcseconds. SOFI = Son of ISAAC. Table 1 is published in its entirety in the electronic edition of the *Astrophysical Journal*. A portion is shown here for guidance regarding its form and content.

^a The robust sample is that with $S/N(z_{850}) > 10$. Objects with $S/N < 10$ should be regarded with caution and may include spurious contaminants (see text).

^b Color limits are reported at 2σ .

UT 2002 October 9 in poor weather conditions and detected line emission at 8303 \AA . Deeper observations (7.8 ks) with the 400 line mm^{-1} grating ($R \approx 1000$) were obtained on UT 2002 November 8. Observations (12 ks) with the FOcal Reducer/low dispersion Spectrograph 2 (FOR2) on the Yepun telescope (VLT 4) were obtained on UT 2002 December 8 with the 3001 grism ($R \approx 860$). We reduced the data with IRAF following standard procedures and combined the LRIS and FOR2 data with appropriate weighting. The final spectrum (Fig. 2, *bottom*) shows $\text{Ly}\alpha$ emission at $z = 5.829$ with flux $1.6 \times 10^{-17} \text{ ergs cm}^{-2} \text{ s}^{-1}$. The blue cutoff, characteristic of high-redshift $\text{Ly}\alpha$, and the $\text{Ly}\alpha$ forest continuum break are clearly evident. The emission line is not seen in the ACS grism spectrum. The ACS exposure time calculator predicts a detection with $S/N \approx 15$ for a point source, but extended emission with a continuum will be harder to detect. We obtained an LRIS spectrum of the only extended HDF-N candidate with $S/N(z_{850}) > 10$ (J123619.9+620934) on UT 2003 May 1 but did not successfully measure a redshift.

4. OTHER CANDIDATE $z \approx 6$ OBJECTS

There are 16 objects with $S/N(z_{850}) > 10$ that meet our selection criteria. Eleven are point sources (3.4% of the stellar objects with $24 < z_{850} < 26.2$; $0''.12 < \text{FWHM} < 0''.16$ vs. $0''.18-$

$0''.7$ for extended $S/N > 10$ candidates), whose $i_{775}-z_{850}$ colors are suspect (§ 2). Deep near-IR imaging from the VLT Infrared Spectrometer And Array Camera (ISAAC) covers $\sim 30\%$ of the GOODS/CDF-S (Giavalisco et al. 2004b), including all three CDF-S stellar i -dropout candidates, whose $z_{850}-J$ colors are redder than expectations for high-redshift objects (Fig. 3). Although some of the eight HDF-N point sources might be at high redshift, we believe that they are probably stars and will not consider them further here. This leaves five extended candidates with $S/N(z_{850}) > 10$, or $0.016 \text{ arcmin}^{-2}$ (Table 1).

Stanway, Bunker, & McMahon (2003, hereafter SBM) used the public release version 0.5 GOODS ACS CDF-S data to identify nine i -dropout candidates. Three are in our sample, and two have been confirmed spectroscopically (Bunker et al. 2003; this Letter). SBM object 5 is unresolved, with the reddest $i_{775}-z_{850}$ color (>2.7 at 2σ) of any GOODS object. Its exceptionally blue near-IR colors ($J-H = -0.3$, $H-K = -0.5$, AB) suggest that it may be a T dwarf (see also SBM). Another point source, SBM object 4, was observed in the GOODS spectroscopic program and is a cool star (approximately L0 V). SBM objects 2, 4, 8, and 9 have $S/N > 2$ in V_{606} and/or B_{435} , are fairly bright in near-IR images, and are thus unlikely to be at $z \sim 6$. SBM object 6 falls outside the area analyzed here, with shallow Viz (and no B_{435}) data. In summary, three (perhaps four) of the nine SBM objects are good $z \sim 6$ candidates.

Data artifacts (space junk trails, reflection ghosts, diffraction spikes, residual cosmic rays) produce spurious z_{850} detections without shorter wavelength counterparts that mimic i -dropouts. We have removed most of these by visual inspection. This is generally easy at $S/N > 10$, but this corresponds to $\langle z_{850} \rangle \approx 25.3$, which is fairly bright for galaxies at $z \approx 6$. Our catalogs push deeper; ex post facto, we truncate them at $S/N \geq 5$ and reject sources that are too small or sharp to be real. However, some spurious sources probably remain. As one check, we masked areas with objects and detected “negative sources.” We find 57 that qualify as i -dropouts. All have $-S/N < 8$, and $\sim 75\%$ have $5 < -S/N < 6$.

The vast majority of real, faint galaxies have $i_{775}-z_{850} < 1.3$ and $z \ll 6$, but measurement errors may scatter a small fraction to redder colors. We estimate this contamination using brighter objects [$S/N(z_{850}) > 20$]. We randomly assign their colors to fainter objects and then perturb the fluxes using the error distributions quantified in § 2. Only approximately two foreground interlopers with $S/N > 10$ would (barely) meet the i -dropout criteria, while ~ 49 objects with $5 < S/N < 10$ could do so. Altogether, possible contaminants represent less than 0.7% of the $\sim 16,000$ GOODS sources with $5 < S/N(z_{850}) < 10$ but may contribute $\sim 45\%$ of the faint $z \sim 6$ candidates. After subtracting the expected contamination, we estimate that there are ~ 145 candidates with $S/N > 5$ (0.46 arcmin^{-2}), more than

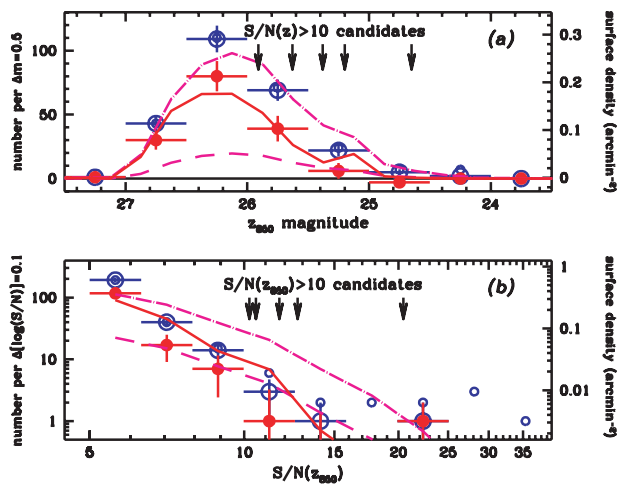


FIG. 4.—Number counts of i -dropout candidates vs. z_{850} magnitude (a) and vs. the S/N of the z_{850} detection image (b). The small and large open circles show “raw” counts with and without point sources. The filled red circles are counts after statistical correction for spurious objects. The vertical error bars show \sqrt{N} counting statistics. The arrows indicate locations for the five most secure candidates. The lines show predicted counts from simulations with various assumptions about the galaxy LF. The dot-dashed line uses the $z = 3$ LBG LF, while the dashed line uses the same L^* but reduces ϕ^* by a factor of 5. The solid line shows the best-fit Schechter function to the corrected $N(z_{850})$ points, with $L^* = 0.4L_{z=3}^*$ and $\phi^* = 3.8\phi_{z=3}^*$.

50% of which have $5 < S/N < 6$. We stress that many of the candidates with $S/N(z_{850}) < 10$ in Table 1 may be spurious or interlopers; this list should be used with caution.

There are four extended candidates with $S/N > 7$ in the portion of the CDF-S with deep ISAAC imaging (Fig. 3). One has red $z_{850}-J$ and bright IR magnitudes and is unlikely to be at $z \approx 6$. Two or perhaps three candidates, including SiD2, are very faint in the near-IR ($24.7 < J_{AB} < 24.9$), with colors expected for galaxies at $5.5 < z < 6$.

5. DISCUSSION

The $i_{775}-z_{850} > 1.3$ limit sets a lower redshift bound for i -dropouts, while IGM suppression in z_{850} makes the upper bound, and hence the sampling volume, a strong function of luminosity. We use simulations (Giavalisco et al. 2004a) to predict the number counts of candidates, including photometric biases. We generated artificial galaxies with a mixture of disk and bulge surface brightness profiles, ellipticities, and orientations. Their sizes were drawn from a lognormal distribution tuned to reproduce measurements at $z \approx 3-5$ (Ferguson et al. 2004). Their spectra have a distribution of UV spectral slopes that matches the observed colors of LBGs at $z \approx 3$ (Adelberger & Steidel 2000). We distributed the galaxies in redshift, modulated their spectra by IGM opacity (Madau 1995), convolved them with ACS point-spread functions, added them to the GOODS images at various magnitudes, and recovered them with SExtractor.

Figure 4 compares the number of candidates with simulations for various assumptions about the UV luminosity function (LF), which we model as a Schechter (1976) distribution with a faint-end slope $\alpha = -1.6$, as measured for LBGs at $z = 3$ (Adelberger & Steidel 2000). The number of *bright* galaxies is smaller at $z \approx 6$ than at $z = 3$ (see also SBM and Lehnert & Bremer 2003 for $z \approx 5.3$ LBGs from ground-based data). The $z = 3$ LF predicts 30 galaxies with $S/N(z_{850}) > 10$ versus $S/N(z_{850}) > 5$ observed, and 26 with $z_{850} < 25$ versus $z_{850} \leq 7$ observed,¹³ and is excluded with a high degree of confidence ($P < 10^{-8}$). A change in the number of bright objects does not require comparable evolution in the total luminosity density of the population since the number of bright sources is exponentially sensitive to the value of L^* . Schechter functions fitted to the counts in Figure 4a favor fainter L^* and higher ϕ^* compared with their values at $z = 3$. Integrating acceptable fits for $M_{1700\text{\AA}} < -19.4$ ($\approx 0.2L_{z=3}^*$), the UV emissivity is similar to that at $z = 3$ [$\rho(L_{z=6})/\rho(L_{z=3}) = 0.77^{+0.29}_{-0.23}$, 95.4% confidence]. However, the fitted L^* -values, and hence most of the inferred ρ_L , are at $z_{850} > 26.4$, where the current data are uncertain. The fit is strongly driven by objects with $5 < S/N < 6.3$ (Fig. 4b). A model with $L_{z=6}^* = L_{z=3}^*$ and 5 times smaller ϕ^* (and ρ_L) is consistent

¹³ Out of seven candidates with $z_{850} < 25$, only one has $S/N(z_{850}) > 10$. The others may be real, but contamination may be substantial.

with the data at bright magnitudes and high S/Ns but drastically underpredicts the counts at low S/N and $z_{850} > 25.5$. Fits excluding the lowest S/N bin leave ρ_L essentially unconstrained.

Two other studies have analyzed i -dropouts from somewhat deeper ACS images. Yan, Windhorst, & Cohen (2003) found 2.3 candidates per arcmin² with $S/N(z_{850}) > 7.2$ in an ACS image with a 1.5 times longer exposure in z_{850} than the three-epoch GOODS data but a 4.9 times longer exposure in i_{775} , and thus more robust color discrimination against interlopers. Their density is 10 times larger than ours at the same S/N threshold. They estimate that their catalogs are 100% complete for $z_{850} \leq 27.5$, whereas ours are only 50% complete for point sources at $z_{850} = 26.7$ (Giavalisco et al. 2004b). Yan et al. (2003) may have underestimated their source fluxes or spurious detection rate, but it is notable that they also find very few bright candidates (none with $z_{850} < 26.8$). Bouwens et al. (2003) identified 0.5 candidates per arcmin² with $z_{850} < 27.3$ from imaging (5–20 orbits in z_{850}) covering 46 arcmin². They also find few bright candidates (only one with $z_{850} < 25.5$) and estimate $\rho(L_{z=6})/\rho(L_{z=3}) = 0.6 \pm 0.2$.

In summary, we have identified five spatially extended, $S/N(z_{850}) > 10$ candidates for galaxies at $z \sim 6$ in early GOODS ACS imaging. Two have confirmed redshifts $z \approx 5.8$. There are many fainter candidates, but we estimate that $\sim 45\%$ may be spurious detections or foreground interlopers. The number of robust candidates is smaller than is predicted if the LF were the same as that at $z \approx 3$. Our best estimates find fainter L^* , larger ϕ^* , and moderately smaller ρ_L compared with $z = 3$, but this strongly depends on the number of objects at $z_{850} > 26$, which is as yet poorly measured. Constant L^* with smaller ϕ^* and ρ_L are consistent with the bright counts but greatly underpredict the number of faint sources. The measurements do not require (or robustly exclude) a dramatic change in ρ_L from $z \sim 6$ to 3, especially if L^* is evolving with redshift. Giavalisco et al. (2004a) find only a modest change ($-30\% \pm 10\%$) in the luminosity density from $z = 3$ to $z \approx 5$ where the GOODS LBG sample is much better characterized. Our best estimates are consistent with an extrapolation of those results to $z = 6$, but deeper data are needed for a robust measurement. The final GOODS images are deeper, with fewer contaminating artifacts, and other forthcoming data (e.g., the ACS Ultra Deep Field) will provide tighter constraints on the galaxy population at these highest optically accessible redshifts.

We thank other members of the GOODS team and the staffs at STScI, ESO, and the Keck Observatory, who made this project possible. Support was provided by NASA through grant GO09583.01-96A from STScI, which is operated by AURA, Inc., under NASA contract NAS5-26555. Work by L. A. M. and D. S. was supported by NASA through the *SIRTF* Legacy Science Program, through contract 1224666, issued by JPL, California Institute of Technology, under NASA contract 1407.

REFERENCES

- Adelberger, K. L., & Steidel, C. C. 2000, ApJ, 544, 218
 Bertin, E., & Arnouts, S. 1996, A&AS, 117, 393
 Bouwens, R. J., et al. 2003, ApJ, 595, 589
 Bunker, A. J., Stanway, E. R., Ellis, R. S., McMahon, R. G., & McCarthy, P. J. 2003, MNRAS, 342, L47
 Coleman, G. D., Wu, C.-C., & Weedman, D. W. 1980, ApJS, 43, 393
 Ferguson, H. C., et al. 2004, ApJ, 600, L107
 Fan, X., et al. 2003, AJ, 125, 1649
 Giavalisco, M., et al. 2004a, ApJ, 600, L103
 ———. 2004b, ApJ, 600, L93
 Lehnert, M. D., & Bremer, M. 2003, ApJ, 593, 630
 Madau, P. 1995, ApJ, 441, 18
 Madau, P., Ferguson, H. C., Dickinson, M., Giavalisco, M., Steidel, C. C., & Fruchter, A. 1996, MNRAS, 283, 1388
 Oke, J. B., et al. 1995, PASP, 107, 375
 Riess, A., et al. 2004, ApJ, 600, L163
 Schechter, P. 1976, ApJ, 203, 297
 Stanway, E. R., Bunker, A. J., & McMahon, R. G. 2003, MNRAS, 342, 439 (SBM)
 Steidel, C. C., Giavalisco, M., Pettini, M., Dickinson, M., & Adelberger, K. L. 1996, ApJ, 462, L17
 Yan, H., Windhorst, R. A., & Cohen, S. H. 2003, ApJ, 585, L93